

Using MR thermometry for SAR verification in local pTX applications

Klaus M. Huber¹, Joerg Roland², Johanna Schoepfer¹, Stephan Biber², and Sebastian Martius¹
¹Corporate Technology, Siemens, Erlangen, Germany, ²Healthcare, Siemens, Erlangen, Germany

Introduction

Monitoring local and global SAR is one of the major challenges on the way to the clinical use of parallel TX arrays. Unlike in conventional whole-body RF-excitation, TX arrays may create distinct hot spots inside the human body by constructive interference of respective coil elements driven with individual amplitudes and phases. Usually, SAR estimations are based on numerical simulations with 3D-EM-tools which are rather sophisticated and tend to deliver erroneous results in case of unprecise inputs. Therefore it is essential to verify the simulation results by real measurements. To date, verification is done by complex and time-consuming calorimetric procedures with thermally insulated phantoms, which deliver only integral results and thus do not give information about local SAR distribution. Sometimes, fiber-optic temperature sensors are added to monitor temperature at least at some discrete points inside the phantom.

In combination with thermal therapies - such as high-intensity focused ultrasound or laser-induced interstitial therapy - temperature mapping with MRI is a widely used tool for guiding and monitoring. Although there are several physical effects in MRI that might be used for temperature monitoring the excellent linearity of the proton resonance frequency (PRF) change with temperature and its near independence of tissue type have made PRF-based phase mapping methods the preferred choice.

Using PRF-based MR thermometry to verify SAR-simulations might be a significant improvement compared to calorimetric procedures for its ability to determine spatial temperature maps and thus enabling the localization of hot spots, which is particularly important for qualifying local transmit arrays. The motivation of this study is to examine the feasibility and quantitative accuracy of MR thermometry for SAR and temperature monitoring of local transmit antenna arrays based on existing hardware.

Methods

Due to the temperature dependence both of the volume-magnetic susceptibility and of the electronic-screening constant, the proton resonance frequency (PRF) is also temperature dependent. In literature values of approximately $-0.01 \text{ ppm}/^\circ\text{C}$ for protons in pure water are reported. For the Siemens MAGNETOM Skyra MR scanner used during the experiments this means a PRF shift of about $-1.23 \text{ Hz}/^\circ\text{C}$. When using a gradient echo sequence with an echo time of TE the PRF shift translates to a phase shift of $\Delta\phi/\Delta T = -2\pi \cdot TE \cdot 1.23 \text{ Hz}/^\circ\text{C}$.

All the measurements were carried out with a 1-channel local transmit QED knee coil (15 receive channels). In order to avoid convection, the phantom was filled with agarose water-gel containing 5 g/l of NaCl and 1.25 g/l of NaSO₄. A small reference bottle also filled with water-gel but without any NaCl was placed directly at the side of the phantom. It serves as a reference which is not susceptible to rf-heating due to its low conductivity. In order to cross-check the temperatures derived by the RF heating MR experiment, discrete fiber-optic thermo sensors were placed both on the outside of the phantom and inside the reference bottle.

The thermometry sequence - a segmented gradient echo sequence with echo-planar readout and a TE of 20 ms - automatically accounts for system drifts by referencing the phase variations to a region inside the small reference bottle which is assumed to be kept at constant temperature. Although the reference bottle is not heated by RF, its temperature changes slightly because of indirect heating mainly from the phantom. That is why the results are corrected with the results of fiber sensor #1 in an additional postprocessing step.

Fig. 1: The 2l water-gel phantom is placed inside a local TX knee coil together with a small reference bottle. The figure also shows the positions of the fiber sensors and the region of interest which is used for evaluation of the thermography results.

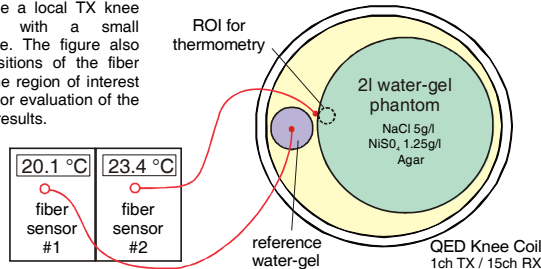


Fig. 2: The MR-scanner with the experimental coil setup

Results

Series of subsequent cycles of RF heating and thermometry sequences have been carried out to observe the effects of RF heating inside the phantom. During heating only rectangular RF pulses with 6 ms pulse width, a repetition rate of 60 ms and a peak power of about 400 W were applied, but no gradients. In fig. 3 the measured temperature maps are shown. Fig. 5 confirms the increased SAR at the outer radius of the phantom caused by the close vicinity to the rods of the knee coil which leads to a non-uniform temperature distribution. Although diffusion should be taken into account for a comparison of the temperature maps with SAR simulation results, MR thermometry proves to be an appropriate means to deliver real-life data to cross-check simulations.

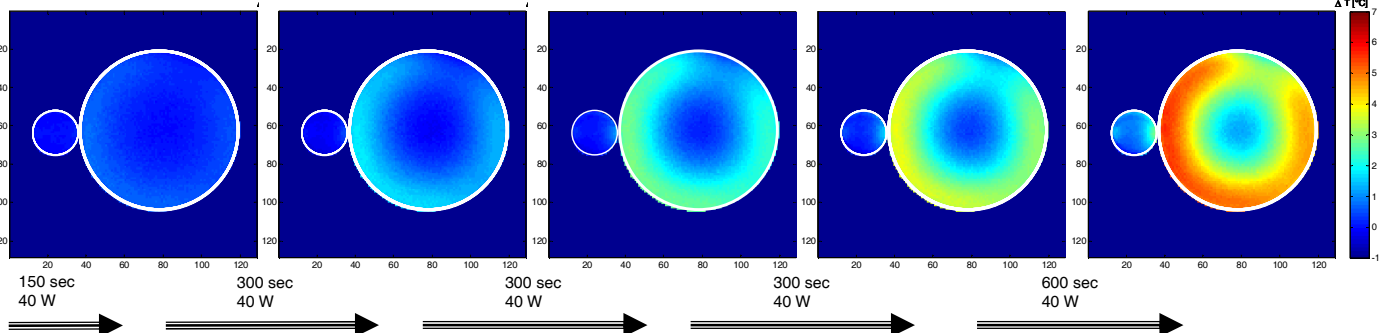


Fig.3: Series of MR thermometry measurements, field of view was $180 \times 180 \text{ mm}^2$ with a voxel size of $1.4 \times 1.4 \times 3.5 \text{ mm}^3$.

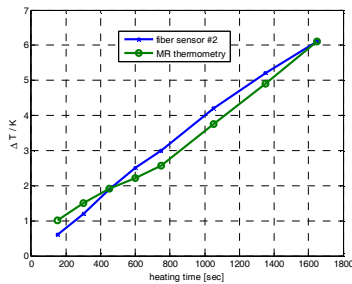


Fig. 4: The thermometry results evaluated in the ROI sketched in fig. 1 are in good agreement with fiber sensor #2.

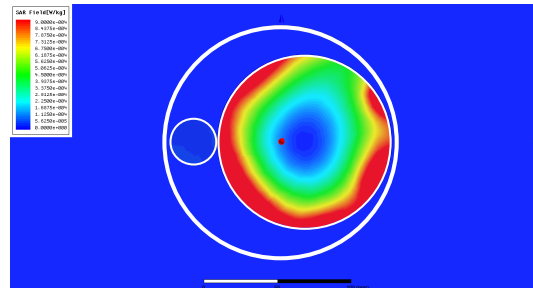


Fig. 5: SAR simulation with Ansys HFSS. The thermometry images (fig. 3) correspond very well to the SAR simulation results, considering that thermometry maps are smoothed due to thermal diffusion.

References: [1] Peters et al, Ex Vivo Tissue-Type Independence in Proton-Resonance Frequency Shift MR Thermometry [2] Rieke et al, MR Thermometry, Journal of Magnetic Resonance Imaging 27:376-390 (2008) [3] Rothgang et al, Automatic B0 Drift Correction for MR Thermometry, Proc. Intl. Soc. Mag. Reson. Med. 19 (2011) [4] Oliver-Taylor et al, Improving SNR in small temperature change MR thermometry to acquire SAR Maps of a pair of ASL Labelling Coils, Proc. Intl. Soc. Mag. Reson. Med. 20 (2012)